

## Solvent Effect on the Singlet Excited-State Lifetimes of Nucleic Acid Bases: A Computational Study of 5-Fluorouracil and Uracil in Acetonitrile and Water

Fabrizio Santoro,<sup>†</sup> Vincenzo Barone,<sup>‡</sup> Thomas Gustavsson,<sup>§</sup> and Roberto Improta<sup>\*,†,||</sup>

Contribution from the Istituto per i Processi Chimico-Fisici del CNR, Area della Ricerca del CNR di Pisa, via Moruzzi 1, I-56124 Pisa, Italy, Dipartimento di Chimica, Università Federico II, Complesso Universitario Monte S. Angelo, Via Cintia, I-80126 Napoli, Italy, Laboratoire Francis Perrin, CEA/DSM/DRECAM/SPAM–CNRS URA 2453, CEA Saclay, F-91191 Gif-sur-Yvette, France, and Istituto di Biostrutture e Bioimmagini-CNR, Via Mezzocannone 6 I-80134 Napoli, Italy

Received August 9, 2006; E-mail: robimp@unina.it

**Abstract:** The first comprehensive quantum mechanical study of solvent effects on the behavior of the two lowest energy excited states of uracil derivatives is presented. The absorption and emission spectra of uracil and 5-fluorouracil in acetonitrile and aqueous solution have been computed at the time-dependent density-functional theory level, using the polarizable continuum model (PCM) to take into account bulk solvent effects. The computed spectra and the solvent shifts provided by our method are close to their experimental counterpart. The  $S_0/S_1$  conical intersection, located in the presence of hydrogen-bonded solvent molecules by CASSCF (8/8) calculations, indicates that the mechanism of ground-state recovery, involving out-of-plane motion of the 5 substituent, does not depend on the nature of the solvent. Extensive explorations of the excited-state surfaces in the Franck–Condon (FC) region show that solvent can modulate the accessibility of an additional decay channel, involving a dark  $n/\pi^*$  excited state. This finding provides the first unifying explanation for the experimental trend of 5-fluorouracil excited-state lifetime in different solvents. The microscopic mechanisms underlying solvent effects on the excited-state behavior of nucleobases are discussed.

### 1. Introduction

DNA photodamage is a phenomenon of fundamental biological importance<sup>1–3</sup> that is modulated by several kinds of microscopic processes related to the intrinsic characteristics of its constituents (nucleobases, nucleosides, and nucleotides) or to their interaction in the DNA double helix, via base stacking or base pairing. The rapid advances in time-resolved spectroscopic techniques and in the excited states quantum mechanical calculations have provided fundamental insights about the photophysical behavior of isolated nucleobases, suggesting possible deactivation paths responsible for the ultrafast radiationless decay of their excited states.<sup>4–32</sup> At the same time, important aspects of the excited-state dynamics in single and

double strand oligonucleotides started being assessed.<sup>33–35</sup> In particular, there have been important advances in the understanding of intramolecular effects on the excited-state dynamics of nucleobases such as uracil and thymine,<sup>17–23</sup> cytosine,<sup>10,24–26</sup> adenine,<sup>22,27–31</sup> and guanine-cytosine basepairs.<sup>36–38</sup>

<sup>†</sup> Istituto per i Processi Chimico-Fisici del CNR.

<sup>‡</sup> Università Federico II.

<sup>§</sup> Laboratoire Francis Perrin.

<sup>||</sup> Istituto di Biostrutture e Bioimmagini-CNR.

- (1) Crespo-Hernandez, C. E.; Cohen, B.; Hare, P. M.; Kohler, B. *Chem. Rev.* **2004**, *104*, 1977–2020.
- (2) Bensasson, R. V.; Land, E. J.; Truscott, T. G. *Excited states and free radicals in Biology and Medicine*; Oxford University Press: Oxford, 1993.
- (3) Sinha, R. P.; Häder, D.-P. *Photochem. Photobiol. Sci.* **2002**, *1*, 225–236.
- (4) Pecourt, J.-M. L.; Peon, J.; Kohler, B. *J. Am. Chem. Soc.* **2000**, *122*, 9348–9349.
- (5) Pecourt, J.-M. L.; Peon, J.; Kohler, B. *J. Am. Chem. Soc.* **2001**, *123*, 10370–10378.
- (6) Cohen, B.; Hare, P. M.; Kohler, B. *J. Am. Chem. Soc.* **2003**, *125*, 13594–13601.

- (7) Malone, R. J.; Miller, A. M.; Kohler, B. *Photochem. Photobiol.* **2003**, *77*, 158.
- (8) Cohen, B.; Crespo-Hernandez, C. E.; Kohler, B. *Faraday Discussions of the Chemical Society* **2004**, *127*, 137–147.
- (9) Crespo-Hernández, C. E.; Kohler, B. *J. Phys. Chem. B* **2004**, *108*, 11182–11188.
- (10) Blancafort, L.; Cohen, B.; Hare, P. M.; Kohler, B.; Robb, M. A. *J. Phys. Chem. A* **2005**, *109*, 4431–4436.
- (11) Peon, J.; Zewail, A. H. *Chem. Phys. Lett.* **2001**, *348*, 255–262.
- (12) Gustavsson, T.; Sharonov, A.; Markovitsi, D. *Chem. Phys. Lett.* **2002**, *351*, 195–200.
- (13) Gustavsson, T.; Sharonov, A.; Onidas, D.; Markovitsi, D. *Chem. Phys. Lett.* **2002**, *356*, 49–54.
- (14) Onidas, D.; Markovitsi, D.; Marguet, S.; Sharonov, A.; Gustavsson, T. *J. Phys. Chem. B* **2002**, *106*, 11367–11374.
- (15) Sharonov, A.; Gustavsson, T.; Carré, V.; Renault, E.; Markovitsi, D. *Chem. Phys. Lett.* **2003**, *380*, 173–180.
- (16) Pancur, T.; Schwalb, N. K.; Renth, F.; Temps, F. *Chem. Phys.* **2005**, *313*, 199–212.
- (17) Improta, R.; Barone, V. *J. Am. Chem. Soc.* **2004**, *126*, 14320–14321.
- (18) Gustavsson, T.; Banyasz, A.; Lazzarotto, E.; Markovitsi, D.; Scalmani, G.; Frisch, M. J.; Barone, V.; Improta, R. *J. Am. Chem. Soc.* **2006**, *128*, 607–619.
- (19) Gustavsson, T.; Sarkar, N.; Lazzarotto, E.; Markovitsi, D.; Barone, V.; Improta, R. *J. Phys. Chem. B* **2006**, *110*, 12843–12847.
- (20) Gustavsson, T.; Sarkar, N.; Lazzarotto, E.; Markovitsi, D.; Improta, R. *Chem. Phys. Lett.* **2006**, *429*, 551–557.
- (21) Matsika, S. *J. Phys. Chem. A* **2004**, *108*, 7584–7590.

Even if each compound exhibits a different decay mechanism, some common features can be highlighted. In all of the above compounds a very low barrier ( $\sim 0.1$  eV,  $\sim 800$  cm $^{-1}$ ) should separate the minimum of the bright state (arising from a  $\pi/\pi^*$  transition, hereafter  $S_\pi$ ) from an easily accessible conical intersection (CI) with the ground state ( $S_0$ ). Out-of-plane deformation of a carbon atom in a six-membered ring (with a “perpendicular arrangement” of one of the substituents) has been suggested to be the crucial mechanistic step toward the CI region.<sup>1</sup>

The ultrafast decay is thus explained on the ground of a purely intramolecular mechanism, little or not affected by the solvent. However, the role of environmental effects is far from being assessed. Most of the ultrafast studies have indeed been performed in aqueous solution, whereas the number of comparative studies in different solvents is still limited.<sup>1</sup> With some exceptions,<sup>1</sup> most of the studies do not report any significant dependence of the excited-state lifetimes on the nature of the embedding medium.<sup>6,10</sup>

Recent thorough comparative studies of a series of uracil derivatives in different solvents have provided a very different picture, indicating that the solvent can remarkably modulate the excited-state behavior of nucleobases.<sup>19,20</sup> In fact, time-resolved fluorescence upconversion experiments show that the excited-state lifetimes of thymine and 5-fluorouracil (5FU) in acetonitrile are significantly shorter than in water. Preliminary calculations on 5FU in acetonitrile suggest that an additional decay channel exists for this molecule in acetonitrile, involving a dark  $n/\pi^*$  state (hereafter  $S_n$ ) almost isoenergetic to the  $S_\pi$  state in the Franck–Condon (FC) region.<sup>19</sup> Besides its significance for the excited-states behavior of nucleobases, the possibility that solvent modulates the accessibility of the different decay channels is very important for the study of photoexcited molecules in solution,<sup>39–45</sup> and thus it would be interesting to

verify this hypothesis by state of the art quantum mechanical calculations in the condensed phase. To this aim and to get a more complete picture of solvent effects on the behavior and the lifetimes of uracil excited states, it is necessary to address several basic questions.

First, the role of solvent effects in tuning the behavior of both  $S_\pi$  and  $S_n$  states must be analyzed in deeper detail, especially in the FC region. This means not only to characterize the excited-state  $S_\pi$  and  $S_n$  minima but also to explore the potential energy surfaces (PES) around the path connecting the FC point with the minima. This analysis represents a preliminary but mandatory step toward a dynamical description of the excited-state ground-state recovery. A theoretical treatment is particularly important for the dark  $S_n$  state, since the  $S_0$ – $S_n$  transition cannot be easily characterized by experiments, owing to its vanishingly small oscillator strength. Furthermore, in order to understand at a molecular level the chemical effects underlying the dependence of the excited-state lifetimes on the solvent, it would be important to decompose the “global” solvent effects in its components, for example, discriminating the contributions of solvent polarity and of solute/solvent hydrogen bonds. Such a knowledge would help in understanding the role played by environmental effects in more complex systems, such as, for example, photoexcited nucleic acid strands. Finally, it would be highly desirable to examine the interplay between solvent and substituent effects, performing the same synoptical analysis on different nucleobases.

Most of the above questions are tackled in the present paper. In detail, we study by means of density-functional theory (DFT) and time-dependent density-functional theory (TDDFT) PCM calculations the absorption and the emission spectra of the two lowest excited states of uracil (U) and 5FU, in two different solvents, namely, acetonitrile, a polar but aprotic solvent, and water. We investigate the effect of solute–solvent hydrogen bonds on the mechanism of the radiationless deactivation of the bright  $S_\pi$  state, by locating at the CASSCF level the CI with the ground state in the presence of four water molecules belonging to the first solvation shell. Finally, we perform an extensive exploration of the excited-states PES in the FC region both in acetonitrile and in water, providing strong indications that *the involvement of the dark  $S_n$  state in the photoexcited dynamics does depend on the solvent*. Besides their relevance for the study of the excited-state behavior of nucleobases, our results will provide the ground for a more general discussion about the microscopic mechanisms underlying solvent effects on the dynamics of photoexcited molecules in solution.

## 2. Computational Details

All the calculations have been performed on the diketo form of uracil and 5-fluorouracil. This is the most stable form in the electronic ground state,<sup>46</sup> and the only tautomer identified in solution and in the gas phase.<sup>47,48</sup>

The absorption and emission spectra have been calculated by TDDFT using the PBE0 exchange-correlation functional.<sup>49</sup> Geometry optimiza-

- (22) Matsika, S. *J. Phys. Chem. A* **2005**, *109*, 7538–7545.  
 (23) Zgierski, M. Z.; Patchkovskii, S.; Fujiwara, T.; Lim, E. C. *J. Phys. Chem. A* **2005**, *109*, 9384–9387.  
 (24) (a) Ismail, N.; Blancafort, L.; Olivucci, M.; Kohler, B.; Robb, M. A. *J. Am. Chem. Soc.* **2002**, *124*, 6818–6819. (b) Merchan, M.; Serrano-Andres, L.; Robb, M. A.; Blancafort, L. *J. Am. Chem. Soc.* **2005**, *127*, 1820–1825.  
 (25) Blancafort, L.; Robb, M. A. *J. Phys. Chem. A* **2004**, *108*, 10609–10614.  
 (26) Zgierski, M. Z.; Patchkovskii, S.; Lim, E. C. *J. Chem. Phys.* **2005**, *123*, 081101–081104.  
 (27) Marian, C. M. *J. Chem. Phys.* **2005**, *122*, 104314.  
 (28) Marian, C.; Nolting, D.; Weinkauff, R. *Phys. Chem. Chem. Phys.* **2005**, *7*, 3306–3316.  
 (29) Nielsen, S. B.; Sølling, T. I. *ChemPhysChem* **2005**, *6*, 1276–1281.  
 (30) Perun, S.; Sobolewski, A. L.; Domcke, W. *Chem. Phys.* **2005**, *313*, 107–112.  
 (31) (a) Perun, S.; Sobolewski, A. L.; Domcke, W. *J. Am. Chem. Soc.* **2005**, *127*, 6257–6265. (b) Blancafort, L. *J. Am. Chem. Soc.* **2006**, *128*, 210–219.  
 (32) Canuel, C.; Mons, M.; Piuze, F.; Tardivel, B.; Dimicoli, I.; Elhanine, M. *J. Chem. Phys.* **2005**, *122*, 0743161–0743166.  
 (33) Crespo-Hernández, C. E.; Cohen, B.; Kohler, B. *Nature* **2005**, *436*, 1141–1144.  
 (34) Markovitsi, D.; Onidas, D.; Gustavsson, T.; Talbot, F.; Lazzarotto, E. *J. Am. Chem. Soc.* **2005**, *127*, 17130–17131.  
 (35) Markovitsi, D.; Talbot, F.; Gustavsson, T.; Onidas, D.; Lazzarotto, E.; Marguet, S. *Nature* **2006**, *441*, E7.  
 (36) Sobolewski, A. L.; Domcke, W. *Phys. Chem. Chem. Phys.* **2004**, *6*, 2763–2771.  
 (37) Sobolewski, A. L.; Domcke, W.; Hättig, C. *Proc. Natl. Acad. Sci. U.S.A.* **2005**, *102*, 17903–17906.  
 (38) (a) Tsolakidis, A.; Kaxiras, E. *J. Phys. Chem. A* **2005**, *109*, 2373–2380.  
 (39) Burghardt, I.; Cederbaum, L. S.; Hynes, J. T. *Faraday Discussions* **2004**, *127*, 395.  
 (40) Yamazaki, S.; Kato, S. *J. Chem. Phys.* **2005**, *123*, 114510.  
 (41) Toniolo, A.; Olsen, S.; Manohar, L.; Martinez, T. J. *Faraday Discussions* **2004**, *127*, 149.  
 (42) Sorgues, S.; Mestdagh, J. M.; Soep, B. *Chem. Phys. Lett.* **2004**, *399*, 234.  
 (43) Burghardt, I.; Hynes, J. T.; Gindensperger, E.; Cederbaum, L. S. *Phys. Scr.* **2006**, *73*, C42.

- (44) Muller, A. M.; Lochbrunner, S.; Schmid, W. E.; Fuss, W. *Angew. Chem., Int. Ed.* **1998**, *37*, 505.  
 (45) Fuss, W. *Photochem. Photobiol. Sci.* **2002**, *1*, 255.  
 (46) Marian, C. M.; Schneider, F.; Kleinschmidt, M.; Tatchen, J. *Eur. Phys. J. D* **2002**, *20*, 357–367.  
 (47) Becker, R. S.; Kogan, G. *Photochem. Photobiol.* **1980**, *31*, 5–13.  
 (48) Colarusso, P.; Zhang, K.; Guo, B.; Bernath, P. F. *Chem. Phys. Lett.* **1997**, *269*, 39–48.  
 (49) Adamo, C.; Barone, V. *J. Chem. Phys.* **1999**, *110*, 6158–6170.

tions were performed at the PBE0/6-31G(d) level<sup>49</sup> for the ground electronic states and at the TD-PBE0 6-31G(d) level for the excited states.<sup>50,51</sup> Analytical excited-state geometry optimizations have been performed at the PCM/TD-PBE0/6-31G(d) level in aqueous and acetonitrile solutions,<sup>52</sup> based on the linear response (LR) theory, described in ref 53.

We verified that the Kohn–Sham orbitals mainly involved in the excitations are always very similar to the Hartree–Fock ones computed with the same basis set and are thus suitable for qualitative physical interpretation. We checked that all the computed vibrational frequencies in the minima of the  $S_0$  and excited surfaces are positive.

Conical intersections between the ground and the  $S_\pi$  state have been located in the gas phase at the CASSCF(8/8)/6-31G(d) level, by using the method of Bearpark et al.,<sup>54</sup> including six  $\pi$  molecular orbitals and the two highest energy  $n_o$  valence orbitals (corresponding to lone pairs of the two carbonyl groups). Planar conical intersections between  $S_\pi$  and  $S_n$  states have been located at the CASSCF(6/6)/6-31G(d) level (including five  $\pi$  molecular orbitals and the highest energy  $n_o$  valence orbital). In both cases the CI structures are very similar to those obtained for uracil by Matsika at the MRCI(12/9) level<sup>21,22</sup> (and checked by single-point calculations with larger active spaces) suggesting that our computational approach is fully adequate for the purposes of the present paper, namely, obtaining a good estimate of the CI structure to be used for the subsequent PCM/TD-PBE0 analysis of the PES between the FC and CI structures.

**Solvation Model.** Bulk solvent effects on the ground and the excited states have been taken into account by means of the polarizable continuum model (PCM).<sup>55,56</sup> In this model the molecule is embedded in a cavity surrounded by an infinite dielectric with the dielectric constant of the solvent (we have used standard dielectric constants 36.64 for acetonitrile and 78.39 for water). Ground and excited-state geometry optimizations in solution have been performed using UA0 radii for the solute cavity, complemented by single point energy calculations employing UAHF radii that are expected to provide more accurate solvation energies.<sup>57</sup> Even if small differences can be found between the results obtained using UAHF and UA0 models (as those reported in our previous studies),<sup>18–20</sup> we checked that our results do not qualitatively depend on the choice of the cavity radii.

While PCM can adequately model  $\text{CH}_3\text{CN}$  solution, a proper description of solvent shifts in aqueous solution requires also the explicit inclusion of water molecules belonging to the first solvation shell. Taking into account experimental<sup>58,59</sup> and computational evidence<sup>60</sup> all the PCM calculations for aqueous solution refer to the species  $5\text{FU}\cdot\text{H}_2\text{O}$  and  $\text{U}\cdot\text{H}_2\text{O}$ , where four water molecules of the first solvation shell are explicitly included (see ref 18).

When discussing solvent effects on absorption spectra it is useful to define two limit situations, usually referred to as nonequilibrium and equilibrium time-regimes.<sup>51,55</sup> In the former case, only solvent electronic polarization (fast solvent degrees of freedom) is in equilibrium with the excited-state electron density of the solute, whereas in the equilibrium regime also nuclear polarization (and, thus, both fast and slow solvent degrees of freedom) is equilibrated with the excited-state electron density.

To calculate the vertical excitation energies (VEE), nonequilibrium solvation energies are more suitable, while the opposite is true for fluorescence energies. However, because of the very short excited-state lifetime of the nucleobases it cannot be taken for granted that all the solvent degrees of freedom are at the equilibrium with the excited-state electron density when the emission process occurs. As a consequence, we always report both equilibrium and nonequilibrium fluorescence energies.

Even if a rigorous theoretical procedure for the calculation of state specific (SS) fluorescence energies would require the SS-TD/PCM approach<sup>61</sup> which is still under development, a sufficient degree of accuracy can be obtained by using the emission energies provided by the standard linear response (LR)-TD/PCM implementation.

Upon crossing, adiabatic excited states  $S_1$  and  $S_2$  exchange their  $n/\pi^*$  and  $\pi/\pi^*$  electronic character, as indicated by the variation in the transition dipole moment with the ground state. In such cases the slow dependence on the nuclear coordinates of this latter quantity is used as a key marker to define pseudoadiabatic  $S_\pi$  and  $S_n$  electronic states and to check the “degree of mixing” between them. In this respect, we point out that the two lowest energy excited states always have a clear single-determinant character, which is mandatory for the reliability of a TDDFT computational approach.

All the calculations have been performed by using a development version of the Gaussian package.<sup>62</sup>

### 3. Results

This section is organized as follows. We first present our computed vertical excitation energies (VEE) and the emission energies for 5FU and U in  $\text{CH}_3\text{CN}$  and for  $5\text{FU}\cdot\text{H}_2\text{O}$  and  $\text{U}\cdot\text{H}_2\text{O}$  in aqueous solution. The comparison between our results and the experimental absorption and fluorescence spectra is indeed critical for assessing the reliability of our computational model and will provide useful indications on solvent effects on the relative stability of the  $S_\pi$  and  $S_n$  states. In the next step we focus on the motion toward the CI between  $S_0$  and  $S_\pi$ , analyzing the role of solute solvent hydrogen bonds on the CI structure and comparing the results obtained on U with those concerning 5FU (see ref 19). As a final step we present several 1-dimensional (1D) and 2-dimensional (2D) scans in acetonitrile and in water solution of the excited-state PES in the region connecting the FC point and the minima of the  $S_\pi$  and  $S_n$  states, focusing on the existence and the dynamical relevance of a  $S_\pi/S_n$  crossing.

**3.1. Absorption.**  $S_\pi$  arises mainly from the HOMO  $\rightarrow$  LUMO excitation, with  $\pi/\pi^*$  character, whereas  $S_n$  has a predominant HOMO-1  $\rightarrow$  LUMO character ( $n/\pi^*$ ) (see Figure S1 in the Supporting Information, SI, for a schematic drawing of the relevant orbitals). Confirming the results obtained in aqueous solution by using the UA0 radii in the PCM calculations,<sup>18</sup> the VEE values of the  $S_\pi$  state computed at the PCM/TD-PBE0 level (see Table 1) are in good agreement with the experimental absorption maxima, in spite of a slight general overestimation ( $\sim 3000\text{ cm}^{-1}$  at the 6-31G(d) level and  $\sim 1700\text{ cm}^{-1}$  at the 6-311+G(2d,2p) level for 5F, whereas for U the discrepancy is  $\sim 1000\text{ cm}^{-1}$  larger). It is noteworthy that the experimental values for the water  $\rightarrow$  acetonitrile solvent blue-shift ( $300\text{ cm}^{-1}$  and  $500\text{ cm}^{-1}$  for 5FU and U, respectively) are close to our PCM/TD-PBE0 results. Both the increase of solvent polarity and the formation of solute–solvent hydrogen bonds slightly decrease the HOMO–LUMO gap, giving account of the water

(50) Adamo, C.; Scuseria, G. E.; Barone, V. *J. Chem. Phys.* **1999**, *111*, 2889–2899.

(51) Cossi, M.; Barone, V. *J. Phys. Chem. A* **2000**, *104*, 10614–10622.

(52) Scalmani, G.; Frisch, M. J.; Mennucci, B.; Tomasi, J.; Cammi, R.; Barone, V. *J. Chem. Phys.* **2006**, *124*, 094107.

(53) Cossi, M.; Barone, V. *J. Chem. Phys.* **2001**, *115*, 4708–4717.

(54) Bearpark, M. J.; Robb, M. A.; Schlegel, H. B. *Chem. Phys. Lett.* **1994**, *223*, 269–274.

(55) Tomasi, J.; Mennucci, B.; Cammi, R. *Chem. Rev.* **2005**, *105*, 2999.

(56) Cossi, M.; Scalmani, G.; Rega, N.; Barone, V. *J. Chem. Phys.* **2002**, *117*, 43.

(57) Barone, V.; Cossi, M.; Tomasi, J. *J. Chem. Phys.* **1997**, *107*, 2310.

(58) He, Y.; Wu, C.; Kong, W. *J. Phys. Chem. A* **2004**, *108*, 943–949.

(59) Chahinian, M.; Seba, H. B.; Ancian, B. *Chem. Phys. Lett.* **1998**, *285*, 337–345.

(60) Gaigeot, M.-P.; Sprick, M. *J. Phys. Chem. B* **2004**, *108*, 7458–7467.

(61) Impropa, R.; Barone, V.; Scalmani, G.; Frisch, M. J. *J. Chem. Phys.* **2006**, *124*, 054103.

(62) Frisch, M. J.; et al. In *Gaussian Development Version*, revision D.02; Gaussian, Inc.: Wallingford CT, 2005.



**Table 1.** Computed Vertical Excitation Energies (in Thousands of  $\text{cm}^{-1}$ ) of 5-Fluorouracil and Uracil in  $\text{CH}_3\text{CN}$  and in Water<sup>a</sup>

|                                | $S_\pi$     |                | $S_n$       |                |
|--------------------------------|-------------|----------------|-------------|----------------|
|                                | 6-31G(d)    | 6-311+G(2d,2p) | 6-31G(d)    | 6-311+G(2d,2p) |
| Nonequilibrium                 |             |                |             |                |
| 5 FU in $\text{CH}_3\text{CN}$ | 41.3 (0.16) | 39.7 (0.17)    | 40.2 (0.0)  | 40.2 (0.0)     |
| 5FU·H <sub>2</sub> O in water  | 40.5 (0.18) | 39.1 (0.19)    | 42.8 (0.0)  | 42.8 (0.0)     |
| Equilibrium                    |             |                |             |                |
| 5 FU in $\text{CH}_3\text{CN}$ | 40.7 (0.22) | 39.1 (0.24)    | 40.1 (0.0)  | 40.2 (0.0)     |
| 5FU·H <sub>2</sub> O in water  | 39.6 (0.26) | 38.2 (0.28)    | 42.8 (0.0)  | 42.7 (0.0)     |
| Nonequilibrium                 |             |                |             |                |
| U in $\text{CH}_3\text{CN}$    | 43.3 (0.16) | 41.7 (0.18)    | 39.6 (0.0)  | 39.9 (0.0)     |
| U·H <sub>2</sub> O in water    | 42.5 (0.14) | 41.1 (0.20)    | 42.5 (0.04) | 42.5 (0.0)     |
| Equilibrium                    |             |                |             |                |
| U in $\text{CH}_3\text{CN}$    | 42.7 (0.23) | 41.1 (0.26)    | 39.6 (0.0)  | 39.8 (0.0)     |
| U·H <sub>2</sub> O in water    | 41.7 (0.28) | 40.2 (0.31)    | 42.5 (0.00) | 42.5 (0.0)     |

<sup>a</sup> PCM/TD-PBE0/6-31G(d) calculations on PCM/PBE0/6-31G(d) optimized geometries. Adimensional oscillator strengths are given in parentheses. Experimental absorption maxima (in thousands of  $\text{cm}^{-1}$ ): 5FU, 37.9 ( $\text{CH}_3\text{CN}$ ), 37.6 ( $\text{H}_2\text{O}$ ); U, 39.1 ( $\text{CH}_3\text{CN}$ ), 38.6 ( $\text{H}_2\text{O}$ ).

→ acetonitrile solvent blue-shift. When substituents able to give rise to a hyperconjugative effect (like fluorine) are present in C<sub>5</sub> position, the HOMO–LUMO energy gap decreases and the  $S_0$ – $S_\pi$  transition is red-shifted with respect to uracil.<sup>18</sup> The computed red-shift is slightly larger than the experimental one, but the discrepancy is similar in acetonitrile and in water, suggesting that this result is due to an intrinsic feature of TD-PBE0 calculations. However, when comparing experimental spectra with the results of excited-state calculations, it is worthy to remember that the position of the maximum of an absorption band does not necessarily coincide with the VEE, since it depends also on the Franck–Condon factors between the ground and the excited-state minima.

Inspection of Table 1 shows that the solvent significantly affects the relative stability of the  $S_\pi$  and the  $S_n$  states. As expected, in water the  $n/\pi^*$  transition is indeed destabilized by the presence of explicit hydrogen bonds involving the carbonyl groups. In fact this electronic transition involves the transfer of an electron from the oxygen lone pairs (LP), that can potentially act as hydrogen-bond acceptors, toward the more diffuse  $\pi^*$  molecular orbital, leading to a decrease of the solute–solvent hydrogen-bond strength. The effect of the solvent polarity on the relative stability of the  $S_\pi$  and  $S_n$  states can be rationalized on the grounds of their electric dipole moment. Our computations in  $\text{CH}_3\text{CN}$  predict, indeed, that the dipole moment of  $S_n$  (1.4 and 1.9 D for 5F and U, respectively) is smaller than those of the ground state (5.0 and 5.3 D for 5F and U, respectively) and of  $S_\pi$  (6.8 and 6.1 D for 5F and for U, respectively).

In aqueous solution the  $S_\pi$  state is therefore significantly more stable than the  $S_n$  one both for U and 5FU. On the contrary, in acetonitrile solution the energy ordering between the transitions depend on the adopted basis set for 5FU, while for uracil  $S_n$  is more stable than  $S_\pi$  at all levels of calculation. TD-PBE0/6-311+G(2d,2p) computations indicate that in the gas phase  $S_n$  is more stable than  $S_\pi$  both for 5FU and U.<sup>18</sup> However the energy difference between those two states is significantly larger for uracil. As a consequence, for 5FU the energy of the  $S_\pi$  and  $S_n$  states is much closer in acetonitrile than in water, whereas just the opposite happens for U.

**3.2. Fluorescence.** The  $S_\pi$  minimum (see Figure 1, hereafter  $S_{\pi\text{-min}}$ ) computed in acetonitrile for 5FU and U is very similar

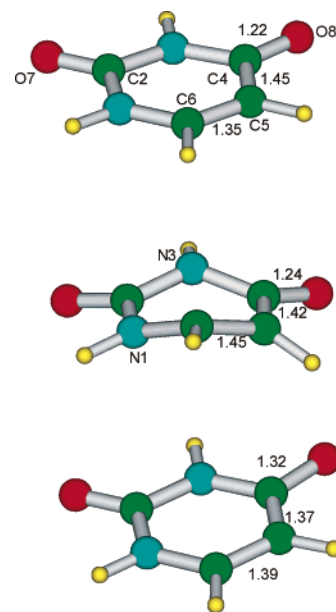


**Figure 1.** Minimum of the  $S_0$  (top),  $S_\pi$  (middle), and  $S_n$  (bottom) states of uracil, according PCM/TD-PBE0-631G(d) excited-state geometry optimizations in acetonitrile. Some selected bond distances (in Å) are also reported.

to that obtained in aqueous solution and already described in ref 18. The pyrimidine ring assumes a “boatlike” conformation, with N<sub>3</sub> and C<sub>6</sub> out of the plane defined by N<sub>1</sub>, C<sub>2</sub>, C<sub>4</sub>, and C<sub>5</sub> that are indeed close to being coplanar (Figure 1). The most relevant changes with respect to the ground-state equilibrium geometry are exhibited by the C<sub>4</sub>C<sub>5</sub>, C<sub>4</sub>O<sub>8</sub>, and, especially, the C<sub>5</sub>C<sub>6</sub> bond lengths. In line with the bonding/antibonding character of HOMO and LUMO with respect to those bonds, the first distance decreases by  $\sim 0.03$  Å, while the second and third ones increase by  $\sim 0.03$  and  $0.1$  Å, respectively. PCM/TD-PBE0 geometry optimizations predict, instead, that the minimum of the  $S_n$  state ( $S_{n\text{-min}}$ ) keeps a planar geometry. The most relevant geometry shifts with respect to the ground-state structure involve the C<sub>4</sub>O<sub>8</sub> and C<sub>5</sub>C<sub>6</sub> bond lengths that increase by  $0.1$  Å and  $0.04$  Å, respectively. The  $n/\pi^*$  transition involves, indeed, the transfer of an electron from an orbital corresponding mainly to the O<sub>8</sub> LP to a  $\pi^*$  orbital localized mainly on the C<sub>5</sub>C<sub>6</sub> and C<sub>4</sub>O<sub>8</sub> bonds.

The structures of the  $S_\pi$  and  $S_n$  energy minima computed in aqueous solution are very similar to those obtained in acetonitrile (see Figure 2). The most significant result of the optimizations in aqueous solution concerns the dependence of the hydrogen-bond distances on the electronic state. Just to take an example, in the optimized  $S_n$  solvation shell the Hw<sub>4</sub>–O<sub>8</sub> hydrogen-bond distance is significantly longer (by  $\sim 0.2$  Å) than in the ground electronic state. This electronic transition decreases the electron population of the O<sub>8</sub> lone pairs, leading to a weakening of the hydrogen bond involving the C<sub>4</sub>O<sub>8</sub> carbonyl group.

Inspection of Table 2 shows that the computed fluorescence energy from the bright state  $S_\pi$  is very close to the experimental emission maximum (around  $30000$   $\text{cm}^{-1}$ ), confirming the accuracy of our computational approach and the reliability of the excited-state geometry optimizations in solution. The agreement between computations and experiments is, however, worse for emission than for absorption. In fact, the fluorescence maximum of 5FU in acetonitrile is slightly red-shifted with respect to aqueous solution, while the opposite result is predicted

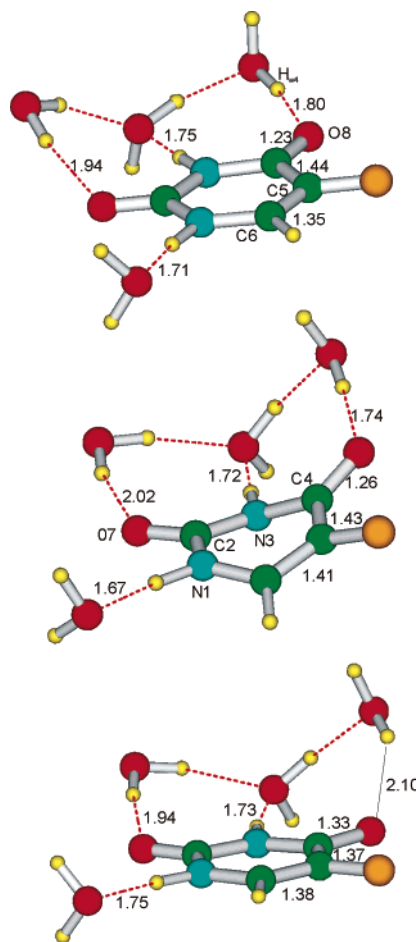


**Figure 2.** Minimum of the  $S_0$  (top),  $S_\pi$  (middle), and  $S_n$  (bottom) states of 5-fluorouracil, according PCM/TD-PBE0-631G(d) excited-state geometry optimizations in water solution. Some selected bond distances (in Å) are also reported.

**Table 2.** Computed Adiabatic Excitation and Vertical Emission Energies (in Thousands of  $\text{cm}^{-1}$ ) of 5-Fluorouracil in  $\text{CH}_3\text{CN}$  and in Water<sup>a</sup>

|                               | 6-31G(d)             |                   | 6-311+G(2d,2p)       |                   |
|-------------------------------|----------------------|-------------------|----------------------|-------------------|
|                               | adiabatic excitation | vertical emission | adiabatic excitation | vertical emission |
| 5FU in $\text{CH}_3\text{CN}$ |                      |                   |                      |                   |
| nonequilibrium                | 37.8 (0.12)          | 30.6              | 36.9 (0.13)          | 29.5              |
| equilibrium                   | 37.2 (0.16)          | 30.0              | 36.2 (0.17)          | 28.9              |
| 5FU·H <sub>2</sub> O in water |                      |                   |                      |                   |
| nonequilibrium                | 37.7 (0.16)          | 32.1              | 36.9 (0.16)          | 31.1              |
| equilibrium                   | 36.8 (0.22)          | 31.2              | 35.9 (0.23)          | 30.2              |
| U in $\text{CH}_3\text{CN}$   |                      |                   |                      |                   |
| nonequilibrium                | 40.0 (0.12)          | 30.0              | 38.9 (0.13)          | 28.9              |
| equilibrium                   | 39.3 (0.16)          | 29.3              | 38.2 (0.18)          | 28.1              |
| U·H <sub>2</sub> O in water   |                      |                   |                      |                   |
| nonequilibrium                | 40.5 (0.16)          | 32.4              | 38.5 (0.16)          | 31.3              |
| equilibrium                   | 39.5 (0.22)          | 31.5              | 37.5 (0.24)          | 30.4              |

<sup>a</sup> PCM/TD-PBE0/6-31G(d) calculations on PCM/PBE0/6-31G(d) optimized geometries. Adimensional oscillator strengths are given in parentheses. Experimental fluorescence energy (in thousands of  $\text{cm}^{-1}$ ): 5FU, 30.0( $\text{CH}_3\text{CN}$ ), 29.4 ( $\text{H}_2\text{O}$ ); U, 30.9 ( $\text{CH}_3\text{CN}$ ) 31.3 ( $\text{H}_2\text{O}$ ).

by our computations, even if the computed emission energies are similar in both solvents. For uracil, experiments and computations agree in predicting a solvent blue-shift between acetonitrile and water, but the computed shift is significantly larger than the experimental one. However, it is always

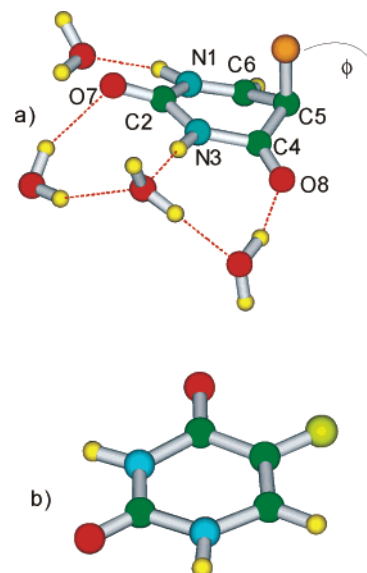


**Figure 3.** (a)  $S_0/S_\pi$  conical intersection for 5-fluorouracil in the presence of four water molecules of the first solvation shell; (b)  $\text{CI}^{0\pi}$  planar conical intersection.

important to recall that when dealing with ultrafast excited-state decay and with broad fluorescence spectra, a quantitative comparison between the computed emission energy and the maximum of the fluorescence band is not straightforward, since the main part of the observed fluorescence spectrum could come from the Franck–Condon region and the excited-state population could be quenched before it reaches  $S_\pi$ -min.

It is important to highlight that our computations indicate that  $S_n$ -min and  $S_\pi$ -min have comparable stabilities both in acetonitrile and in aqueous solution. In the latter case,  $S_n$  is always the most stable excited-state for U, whereas  $S_\pi$  becomes more stable for 5FU in the nonequilibrium regime. However, we emphasize that in aqueous solution the equilibrium solvation shell of the  $S_n$  state exhibits remarkable geometry changes with respect to the ground state, strongly suggesting that this minimum is not relevant in the ultrafast excited-state decay of uracil-like molecules.

**3.3. The Path toward the  $S_0/S_\pi$  Conical Intersection.** In a previous paper we reported the geometry of the lowest energy CI between  $S_0$  and  $S_\pi$  (hereafter  $\text{CI}^{0\pi}$ ) obtained at the CASSCF-(8,8) level<sup>18</sup> for the isolated bases. We have now located  $\text{CI}^{0\pi}$  for the system  $5\text{F}\cdot\text{H}_2\text{O}$  and  $\text{U}\cdot 4\text{H}_2\text{O}$  at the same level of theory (see Figure 3).

It is quite apparent that inclusion of the water molecules does not significantly change the structure of the CI. Confirming previous computational results obtained without including explicitly solvent molecules, one of the key motions to reach  $\text{CI}^{0\pi}$  is the pyramidalization at  $\text{C}_5$ , while an out-of-plane motion (distortion of the planarity of the  $\phi$  dihedral) leads the  $\text{C}_5$  substituent toward a “pseudoperpendicular” arrangement with respect to the molecular plane. When the effect of dynamical electronic correlation is taken into account by TD-PBE0/6-31G-(d) calculations in the gas phase on  $\text{CI}^{0\pi}$ ,  $S_\pi$  and  $S_0$  surfaces are extremely close, their energy difference being smaller than 0.3 eV for all the compounds examined.

Complementing the results already obtained for 5FU,<sup>19</sup> to investigate if an energy barrier exists in the path from FC to CI in uracil too, we have performed PCM/TD-PBE0/6-31G(d)

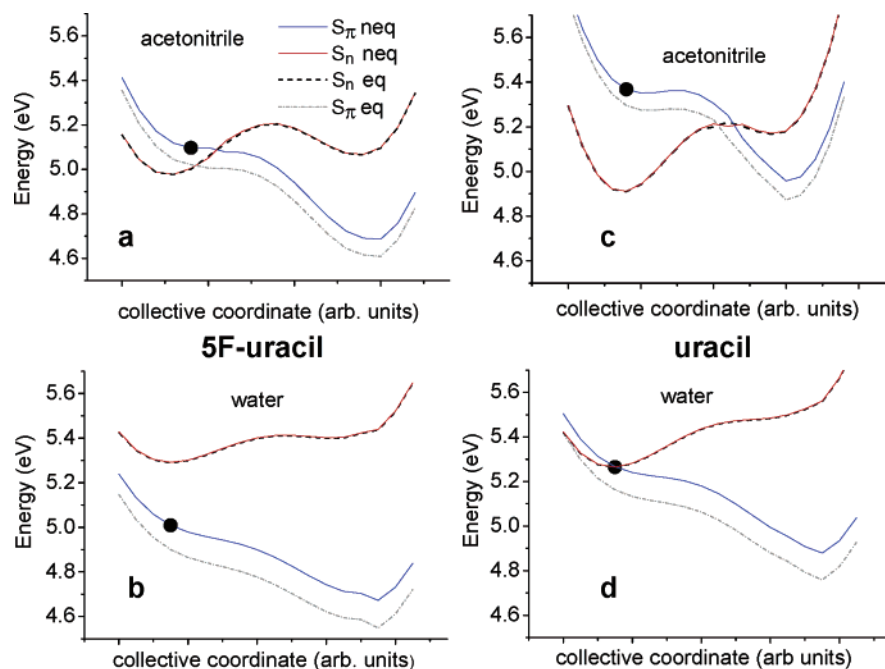


**Figure 4.** (Left) Potential energy surfaces (in eV) of the  $S_n$  and  $S_\pi$  states in the region connecting the FC point and the  $S_\pi$  minimum for 5-fluorouracil: (a) acetonitrile solution; (b) aqueous solution. (Right) Potential energy surfaces (in eV) of the  $S_n$  and  $S_\pi$  states in the region connecting the FC point and the  $S_\pi$  minimum for Uracil: (c) acetonitrile solution; (d) aqueous solution. (PCM/TD-PBE0/6-31G(d) calculations.)

excited-state partial geometry optimizations of U for different values of the  $\phi$  dihedral both in acetonitrile and in aqueous solution (see Figure S2 in the SI). In both solvents our computations confirm the existence of a shallow minimum for  $\phi = 170^\circ$  and then a significant energy increase up to  $\phi \approx 160^\circ$ . For smaller values of the  $\phi$  dihedral, the energy of the  $S_\pi$  state drops, and the geometry starts approaching the CI structure where TD-PBE0 geometry optimizations suffer from severe convergence problems. Nevertheless, a partially relaxed single-point calculation confirms that the energy of  $S_\pi$  decreases with respect to  $\phi \approx 160^\circ$ , suggesting that this point is a saddle point on the isomerization path. The computed energy barriers on the  $S_\pi$  state surface, separating the FC region from the conical intersection, are very similar and extremely small:  $80 \text{ cm}^{-1}$  in aqueous solution and only  $10 \text{ cm}^{-1}$  in acetonitrile solution at the 6-31G(d) level (at the 6-311+G(2d,2p) level the corresponding values are  $100$  and  $40 \text{ cm}^{-1}$ , respectively).

**3.4. Exploring the Excited-State Surfaces in the FC Region.** The analysis of the computed absorption and emission spectra thus suggests that, contrary to what was found in water, an involvement of  $S_n$  in the excited-state dynamics of 5FU and U is possible. To verify this hypothesis and to understand the role played by the solvent, we analyze in some detail the path from the FC point to the  $S_\pi$  minima, both in  $\text{CH}_3\text{CN}$  and in water, computing the one-dimensional (1D) energy profiles of the  $S_\pi$  and  $S_n$  states with respect to a “collective” coordinate  $x$ , defined as a linear interpolation between the internal coordinates of the FC structure and  $S_\pi$ -min (see Figure 4). Restricting the  $3N-6$  dimensional space to a 1D one (or two-dimensional, 2D, vide infra) is clearly arbitrary, and a purposely tailored study of the vibrational modes connecting the FC region to the CI would be necessary in order to unambiguously assess the dynamical motion on the  $S_\pi$  PES. Nevertheless, this procedure can provide a qualitative description of the behavior of the  $S_\pi$  and  $S_n$  states in the first femtoseconds after the excitation. On

the other side, it is noteworthy that even in ground-state reactivity the reaction coordinate is very often a complex and collective coordinate.

The motion on the excited-state surface is certainly accompanied by solvent equilibration to the excited-state electron density. A detailed study of the dynamical coupling between solute and solvent degrees of freedom is outside the scope of the present paper. As a consequence, we will present the PES computed both at the nonequilibrium (neq) and equilibrium (eq) PCM level. The behavior of our system in the first femtoseconds after electron excitation is better described by nonequilibrium calculations, whereas in the proximity of the excited-state minimum the actual nuclear potential is probably intermediate between the two described limits.

Let us start discussing the results obtained for 5FU (Figure 4). In acetonitrile, the energies of the  $S_n$  and  $S_\pi$  states are very close in the first part of the path (within  $0.2 \text{ eV}$ ), and they actually cross quite close to the FC region before reaching  $S_\pi$ -min.

The curves in Figures 4a show a small initial slope suggesting a marginal initial driving-force to distort the ring planarity. Resonance Raman (RR) experiments on 5FU and U indicate that all but one of the vibrational modes more affected by the electronic transition correspond to in-plane stretching and bending,<sup>63,64</sup> suggesting that during the first femtoseconds after the excitation on  $S_\pi$ , uracil-like molecules keep the planar geometry they have at the FC point. We have thus optimized the geometry of the  $S_\pi$  state constraining the pyrimidine ring to planarity ( $S_\pi^{\text{pla}}$ -min see Figure S3 in the SI and Table 3) both in acetonitrile and in water. The path (see Figure 5a) from

(63) Billingham, B. E.; Yeung, R.; Loppnow, G. R. *J. Phys. Chem. A* **2006**, *110*, 6185–6191.

(64) (a) Peticolas, W. R.; Rush, T., III. *J. Comput. Chem.* **1995**, *16*, 1262. (b) Fodor, S. P. A.; Fava, R. P.; Hays, T. R.; Spiro, T. G. *J. Am. Chem. Soc.* **1985**, *107*, 1520.

**Table 3.** Computed Energies (in Thousands of  $\text{cm}^{-1}$ ), Relative to the  $S_0$  Ground States of the Two Lowest Energy States of 5-Fluorouracil in  $\text{CH}_3\text{CN}$  and in Water Solution at the Absolute Minimum, at the Planar Minimum of the  $S_\pi$  State, and at the Planar  $S_\pi/S_n$  Conical Intersection<sup>a</sup>

|                               | absolute $S_\pi$ minimum |             | planar $S_\pi$ minimum |             | planar $S_\pi/S_n$ CI <sup>b</sup> |             |            |
|-------------------------------|--------------------------|-------------|------------------------|-------------|------------------------------------|-------------|------------|
|                               | $S_\pi$                  | $S_n$       | $S_\pi$                | $S_n$       | $S_\pi$                            | $S_n$       |            |
| 5FU in Acetonitrile           | nonequilibrium           | 37.8 (0.12) | 40.8 (0.0)             | 38.9 (0.18) | 39.4 (0.0)                         | 41.1 (0.18) | 41.0 (0.0) |
|                               | equilibrium              | 37.2 (0.16) | 40.8 (0.0)             | 38.2 (0.23) | 39.4 (0.0)                         | 40.3 (0.23) | 41.4 (0.0) |
| 5FU·H <sub>2</sub> O in Water | nonequilibrium           | 37.7 (0.16) | 43.0 (0.0)             | 38.6 (0.18) | 41.9 (0.0)                         |             |            |
|                               | equilibrium              | 36.8 (0.22) | 42.9 (0.0)             | 37.0 (0.26) | 41.9 (0.0)                         |             |            |

<sup>a</sup> PCM/TD-PBE0/6-31G(d) calculations. Adimensional oscillator strengths are given in parentheses; CASSCF/6-31G(d) optimized geometries.

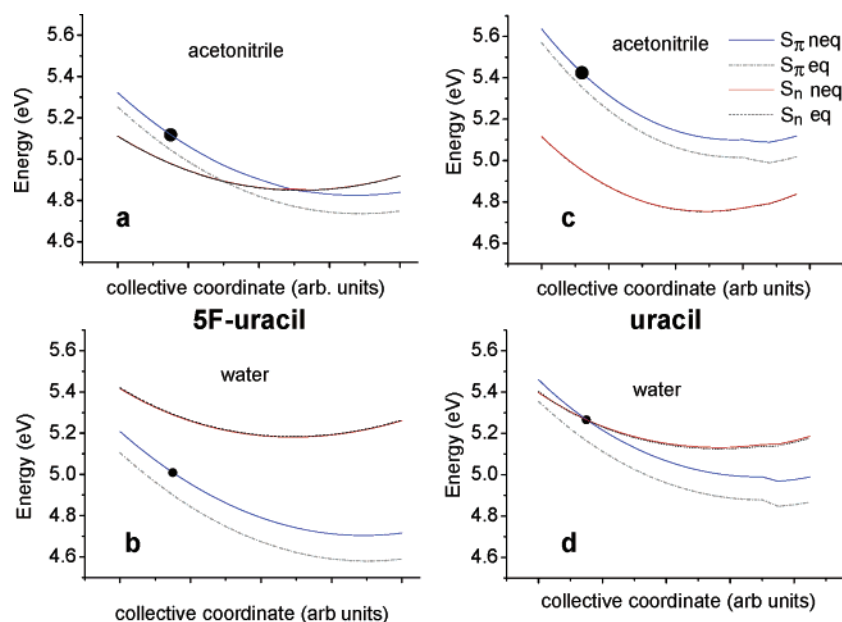


**Figure 5.** (Left) Potential energy surfaces (in eV) of the  $S_n$  and  $S_\pi$  states in the region connecting the FC point and the planar  $S_\pi$  minimum for 5-fluorouracil: (a) acetonitrile solution; (b) aqueous solution. (Right) Potential energy surfaces (in eV) of the  $S_n$  and  $S_\pi$  states in the region connecting the FC point and the planar  $S_\pi$  minimum for uracil: (c) acetonitrile solution; (d) aqueous solution. (PCM/TD-PBE0/6-31G(d) calculations.)

FC to  $S_\pi^{\text{pla-min}}$ , described according to the same procedure followed above, is steeper than the one to  $S_\pi$ -min, thus indicating that  $S_\pi^{\text{pla-min}}$  could be involved in the  $S_\pi$  dynamics.

A crossing between  $S_\pi$  and  $S_n$  is predicted also along the planar path. Moreover, along the path toward the nonplanar minimum,  $S_\pi$  and  $S_n$  have similar stability only in the proximity of the FC region, whereas approaching  $S_\pi$ -min,  $S_\pi$  becomes significantly more stable than  $S_n$ . On the contrary, along the planar path,  $S_\pi$  and  $S_n$  exhibit always a comparable stability, increasing the possibility that the wave packet on  $S_\pi$  is trapped in the  $S_n$  dark state.

Figure 4 and 5 strongly suggest the existence of a conical intersection between  $S_\pi$  and  $S_n$  states for 5FU in acetonitrile. CASSCF calculations indeed predict that a planar-structure CI between the  $S_n$  and the  $S_\pi$  state (hereafter CI<sup>pr</sup>) does exist in vacuo<sup>21</sup> (see Figure 3). PCM/TD-PBE0 calculations in acetonitrile confirm that this structure is representative of the CI present in  $\text{CH}_3\text{CN}$  solution too, since the energy difference between the two states is lower than  $1000 \text{ cm}^{-1}$  (see Table 3).

The picture obtained for 5FU in aqueous solution is completely different (Figure 4b and 5b). Confirming the indications of the computed absorption and fluorescence spectra, the 1D energy profiles suggest that in such a solvent the dynamics on  $S_\pi$  is not influenced to a large extent by  $S_n$ , since this latter is

significantly less stable along the whole path from the FC to the  $S_\pi$ -min. Interestingly, in  $\text{H}_2\text{O}$  the path toward  $S_\pi$ -min is steeper than in acetonitrile and has a slope similar to that of the planar path. As a further check of the likelihood of a  $S_\pi/S_n$  crossing for 5FU in water, we have performed a calculation on CI<sup>pr</sup> adding four water molecules of the first solvation shell. The  $S_\pi$  state is more stable than  $S_n$  by 0.35 eV, thus ruling out the presence of a CI between these two states in aqueous solution.

The 1D energy profiles for uracil sketch a different scenario (Figure 4c,d and 5c,d and Table 4). Indeed, for U  $S_\pi$  and  $S_n$  are closer in water than in acetonitrile. As a consequence, in this latter solvent a crossing between the two states is predicted in a region quite distant from the FC point, whereas in the former the two states cross in the FC region. As for the 5FU case in  $\text{CH}_3\text{CN}$ , the path toward the planar minimum  $S_\pi^{\text{pla-min}}$  is steeper, and in this case at planar configuration the two electronic surfaces remain well apart ( $S_n$  being the more stable).

In order to discriminate the relative importance of bulk solvent effect and of explicit solute/solvent hydrogen bonds we repeated the 1D scan of 5FU from FC to  $S_\pi^{\text{pla-min}}$  by imposing on acetonitrile either the same dielectric constant of water (78.39) or a dielectric constant of 4.0 to mimic a nonpolar solvent (see Figure 6). Inspection of Figure 6 indicates that the polarity of



**Table 4.** Computed Energies (in Thousands of  $\text{cm}^{-1}$ ), Relative to the  $S_0$  Ground States of the Two Lowest Energy States of Uracil in  $\text{CH}_3\text{CN}$  and in Water Solution at the Absolute and at the Planar Minimum of the  $S_\pi$  State<sup>a</sup>

|                                    | absolute $S_\pi$ minimum |            | planar $S_\pi$ minimum |            |
|------------------------------------|--------------------------|------------|------------------------|------------|
|                                    | $S_\pi$                  | $S_n$      | $S_\pi$                | $S_n$      |
| U Acetonitrile                     |                          |            |                        |            |
| nonequilibrium                     | 40.0 (0.12)              | 41.8 (0.0) | 41.1 (0.18)            | 38.5 (0.0) |
| equilibrium                        | 39.3 (0.16)              | 41.8 (0.0) | 40.5 (0.24)            | 38.5 (0.0) |
| U·4H <sub>2</sub> O Water Solution |                          |            |                        |            |
| nonequilibrium                     | 40.5 (0.16)              | 44.3 (0.0) | 41.0 (0.17)            | 42.2 (0.0) |
| equilibrium                        | 39.5 (0.22)              | 44.3 (0.0) | 40.0 (0.27)            | 42.1 (0.0) |

<sup>a</sup> PCM/TD-PBE0/6-31G(d) calculations. Adimensional oscillator strengths are given in parentheses.

the solvent affects the relative position of the two states shifting the crossing-point: the more polar is the environment the closer to the FC region  $S_\pi$  and  $S_n$  states cross. Nonetheless, comparison with Figure 5a,b shows that the potential energy curves change more drastically upon explicit inclusion of water molecules (specifically the destabilization of  $S_n$  increases) thus suggesting that the solute–solvent hydrogen bonds play a role more important than the solvent polarity.

With the aim of exploring more thoroughly the excited-state PES in the region connecting the FC to the excited-state minima, we computed at the PCM/TD-PBE0/6-31G(d) level some bidimensional (2D) maps of the  $S_\pi$  and  $S_n$  surfaces for 5FU in acetonitrile and for 5FU·H<sub>2</sub>O in water (see Figure 7). To build each map, we consider two molecular structures chemically relevant for the dynamics and choose two suitable coordinates to explore the part of the  $S_\pi$  surface which connects them. Because of the tendency to initially preserve the planar geometry, evidenced in Figure 4 and suggested by the RR experiments, we study the path toward the planar minimum  $S_{\pi}^{\text{pla-min}}$ . The comparison between the geometry of the FC point and the  $S_{\pi}^{\text{pla-min}}$  suggests that a relevant coordinate is the  $\text{C}_5\text{C}_6$  bond length, which elongates by 0.08 Å. As a second coordinate, we choose the “collective” coordinate  $x$  defined as imposing that all the other internal coordinates except  $\text{C}_5\text{C}_6$  bond length move from one structure to the other in a synchronous way (linear interpolation).

Inspection of Figure 7 suggests that once excited on  $S_\pi$  at FC, the system feels an acceleration toward  $S_{\pi}^{\text{pla-min}}$  and moves simultaneously along both  $x$  and  $\text{C}_5\text{C}_6$ , confirming that vibrational modes involving  $\text{C}_5\text{C}_6$  stretching should be perturbed by the electronic transition. This prediction is in agreement with that provided by RR experiments.<sup>63,64</sup> In acetonitrile, the  $S_\pi$  and  $S_n$  surfaces intersect along a line which crosses the path followed by the system. This does not happen in aqueous solution because of the strong destabilization of  $S_n$ . Even if further work by using more sophisticated post-SCF ab initio computations is necessary to characterize the  $S_\pi/S_n$  crossing, Figure 7 clearly shows how the solvent qualitatively changes the excited states PES for 5F. The analysis of the path toward  $S_{\pi}^{\text{pla-min}}$  provides similar indications, see Figure S4 in the SI.

It is noteworthy that the coordinate  $x$  mainly involves the  $\text{H}_{12}\text{C}_6\text{N}_1$  and  $\text{H}_7\text{N}_1\text{C}_2$  bendings, which are exactly the motions evidenced by RR experiments in aqueous solution.<sup>63</sup> In this respect our calculations predict some interesting differences between the behavior in acetonitrile and in water, that call for an experimental verification by means of RR experiments in acetonitrile. For example, in water the  $\text{H}_{12}\text{C}_6\text{N}_1$  ( $2.1^\circ$ ) and

$\text{H}_7\text{N}_1\text{C}_2$  ( $2.2^\circ$ ) motions have similar amplitudes. In acetonitrile the situation is somewhat different with an increased motion along  $\text{H}_{12}\text{C}_6\text{N}_1$  ( $3.2^\circ$ ) and a reduced motion along  $\text{H}_7\text{N}_1\text{C}_2$  ( $0.05^\circ$ ). Apart from the bending of the ring atoms, our calculations also predict that in  $\text{CH}_3\text{CN}$  there is a significant motion along the  $\text{F}_{11}\text{C}_5\text{C}_6$  bending ( $4.9^\circ$ ) that is almost completely quenched in water (only  $0.07^\circ$ ).

When the system reaches the crossing point, part of the  $S_\pi$  population could be transferred to  $S_n$  provided that the two states are coupled (and qualitative arguments indicate that this is possible along nonplanar coordinates, where the two electronic states do not have anymore different symmetry). The relevance of such a transfer and whether it is transient or permanent depends on the possible existence on  $S_n$  of an accessible path to drive the system away from the  $S_n/S_\pi$  interaction region. To investigate this possibility, we have explored the surface connecting the  $S_\pi$  planar minimum and the  $S_n$  minimum. A relevant coordinate for a 2D mapping of this region is the  $\text{C}_4\text{O}_8$  bond-length which changes by 0.08 Å between the two minima while, once again, the other coordinate describes a synchronous motion of all the other internal coordinates. Inspection of Figure 8 shows that after the intersection the part of the wavepacket moving on  $S_n$  is accelerated toward the minimum  $S_{n\text{-min}}$ , reaching a region where the  $S_\pi/S_n$  interaction is expected to be negligible because of the energy gap among them. Furthermore, starting from FC the system moves on  $S_\pi$  elongating the  $\text{C}_4\text{O}_8$  bond (which is  $\sim 0.03$  Å longer at  $S_{\pi}^{\text{pla-min}}$  than at FC), and therefore when it reaches  $\text{CI}^{\text{tr}}$  at least a component of its momentum is oriented in the right direction to reach  $S_{n\text{-min}}$ . RR experiments show that this vibrational mode is strongly activated by the  $S_0$ – $S_\pi$  excitation and the path toward both  $S_\pi$  minimum and  $\text{CI}^{\text{tr}}$  involves motion on this mode. Once reached, the minimum of the  $S_n$  dark state in the system can decay nonradiatively to the  $S_0$  state.

The mechanism of ground-state recovery from the  $S_n$  state is still under investigation. In agreement with the picture obtained on cytosine,<sup>24a</sup> preliminary calculations predict that elongation of the  $\text{C}_4\text{O}_8$  bond and out-of-plane motion of the carbonyl group should be involved in this process. The results of a very recent experimental study on an uracil derivative<sup>65</sup> suggest that the excited-state lifetime of the  $S_n$  state is sensitive to the presence of solute/solvent hydrogen bonds (confirming the involvement of the carbonyl group in the ground-state recovery), whereas it does not significantly depend on the polarity of the embedding medium, making less likely the involvement of a charge transfer state in the  $S_n$  decay.

## 4. Discussion

**4.1. Solvent Effects on the Excited-State Behavior of Uracil Derivatives.** As anticipated in the Introduction, the excited-state decay of uracil derivatives is significantly modulated by the nature of the solvent: excited-state lifetimes observed in acetonitrile are indeed substantially shorter than those observed in aqueous solution. This feature is particularly evident for 5FU, the compound exhibiting the longest excited-state lifetime among 11 different uracil derivatives, whose fluorescence decays 3.5 times faster in acetonitrile than in water, decreasing from 1.4 to 0.4 ps.<sup>19</sup>

(65) Hare, P. M.; Crespo-Hernandez, C. E.; Kohler, B. J. *Phys. Chem. B* **2006**, *110* 18641–18650.



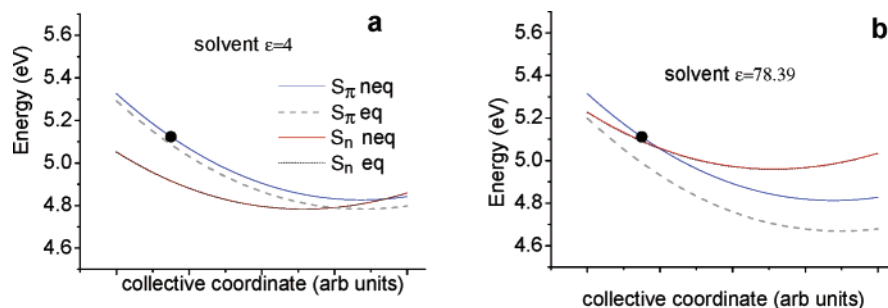


**Figure 6.** Potential energy surfaces (in eV) of the  $S_n$  and  $S_\pi$  states in the region connecting the FC point and the planar  $S_\pi$  minimum for 5-fluorouracil for two embedding medium of different polarity: PCM/TD-PBE0/6-31G(d) calculations.

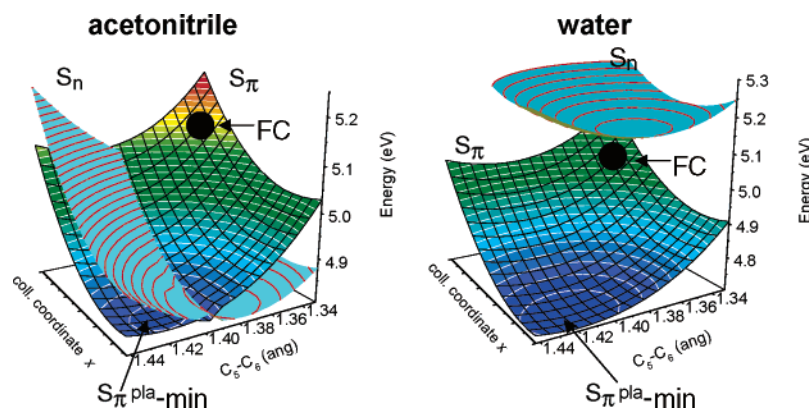


**Figure 7.** Energy of the  $S_\pi$  and  $S_n$  states in the region connecting the FC point and the minimum on  $S_\pi$ : left, acetonitrile solution; right, water solution. (PCM/TD-PBE0/6-31G(d) calculations.)

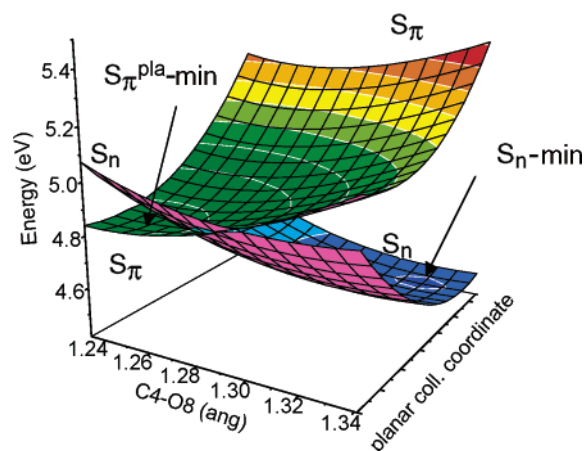


**Figure 8.** Energy of the  $S_\pi$  and  $S_n$  states in the region connecting  $S_\pi$  planar minimum and the  $S_n$  minimum in acetonitrile solution: PCM/TD-PBE0/6-31G(d) calculations.

The comparison of the computational results obtained for 5FU in acetonitrile and in aqueous solution (see also ref 18) strongly suggests that the solvent tuning of the  $S_\pi$  lifetime is mainly due to the modulation of the relative energy of the  $S_\pi$  and the close lying  $S_n$  dark state. In acetonitrile solution, the two states have a comparable stability in a wide portion of the PES in the proximity of the FC region, and the presence of a planar  $S_n/S_\pi$  CI in the proximity of the FC region is very likely (see Figures 4–8), providing another effective decay channel for the wave packet on  $S_\pi$  and leading to a decrease of its experimental lifetime. This extra decay channel should instead not be available in aqueous solution, where  $S_\pi$  is always significantly more stable than  $S_n$ .

According to our calculations on 5FU, the energy difference

between  $S_\pi$  and  $S_n$  states, and thus the excited-state lifetime, increases with the hydrogen-bonding power of the embedding medium. The dependence on the polarity of the embedding medium is comparatively less important, even if in polar solvents the  $S_n/S_\pi$  crossing occurs closer to the FC region, and it could be more effective, since the wavepacket on  $S_\pi$  has a smaller kinetic energy.

The proposal that the excited-state lifetime of 5FU is decreased by the availability of the  $S_\pi/S_n$  decay channel suggests that in alcohols it is intermediate between that found in acetonitrile and that in water (the solvent exhibiting the strongest hydrogen bonds). In nonpolar/non-hydrogen-bonding solvents it should instead be longer than in acetonitrile but shorter than in water. This is confirmed by preliminary time-resolved fluorescence upconversion experiments<sup>66</sup> that we performed in methanol, ethanol, and dioxane that predict the following order for the excited-state lifetime of 5FU:

acetonitrile < dioxane < methanol ~ ethanol < water

Interestingly, the same effect, that is, the relative destabilization of the  $S_n$  state in the presence of solute–solvent hydrogen bonds, produces opposite results for Uracil. Because of the substituent effect in the gas phase, the relative stability of  $S_n$  with respect to  $S_\pi$  is larger for U than for 5FU. As a consequence, when considering the solvent effect, the  $S_\pi$  and  $S_n$  states of U in the FC region are closer in water than in acetonitrile (where  $S_n$  is more stable). Unfortunately, it has not been possible to verify by time-resolved fluorescence experiments whether this leads to longer excited-state lifetimes in

(66) Gustavsson, T.; Sarkar, N.; Lazzarotto, E.; Markovitsi, D.; Barone, V.; Improta, R. In preparation.

aqueous solution since the fluorescence of Uracil is too fast for the experimental time-resolution both in H<sub>2</sub>O and in acetonitrile.

The importance of the interplay between substituent and environmental effects is pointed out, though indirectly, by the fluorescence upconversion experiments performed on thymine. In fact it is significant that, although also for thymine the fluorescence lifetime in CH<sub>3</sub>CN is shorter than in water (235 vs 388 fs), its decrease is significantly lower than for 5FU. This finding can be related to the gas-phase relative stability of S<sub>n</sub> and S<sub>π</sub> states of thymine (~1500 cm<sup>-1</sup>), which is intermediate between that found in uracil (~3600 cm<sup>-1</sup>) and 5-fluorouracil (~1200 cm<sup>-1</sup>).

The S<sub>π</sub>/S<sub>n</sub> decay channel could be effective also in the gas phase or in apolar solvents, where the relative stability of the S<sub>n</sub> state is larger than in CH<sub>3</sub>CN. As a matter of fact, experimental results on thymine in the gas phase indicate that, following the S<sub>π</sub>/S<sub>n</sub> decay at CI<sup>ππ</sup>, the system is trapped in a dark state.<sup>58</sup>

The 1D and 2D maps suggest that upon excitation to S<sub>π</sub>, in the FC region the system experiences a marginal driving force toward distortion from planarity, and moves toward S<sub>π</sub><sup>pla</sup>-min mainly elongating the C<sub>5</sub>C<sub>6</sub> bond. In acetonitrile it reaches a S<sub>π</sub>/S<sub>n</sub> planar conical intersection CI<sup>ππ</sup> where it can either remain on S<sub>π</sub>, progressively acquiring momentum toward the absolute minimum S<sub>π</sub>-min, or make a transition to S<sub>n</sub>, where it accelerates toward the minimum S<sub>n</sub>-min, mainly stretching the C<sub>4</sub>O<sub>8</sub> bond. The part of the wave packet that remains on S<sub>π</sub> eventually moves toward the CI<sup>0π</sup> with S<sub>0</sub> mainly along a flipping motion of the 5-substituent. Even if in principle such motion could modify the electronic structure of S<sub>π</sub> and thus depend on the solvent polarity, our calculations on uracil indicate that, in analogy with 5FU, the energy barrier on S<sub>π</sub> separating the FC region from the CI is very similar in CH<sub>3</sub>CN and in H<sub>2</sub>O. Actually for uracil the energy barrier is almost vanishing, and it is smaller than that found for 5FU (~0.15 eV).<sup>19</sup> This result further supports our explanation of the longer excited-state lifetimes of 5FU, that is, that the out-of-plane motion of the 5-substituent necessary to reach the CI is more difficult for 5FU than for U.

**4.2. Microscopic Basis of Solvent Effect on the Excited Behavior of Nucleobases.** The case of uracil provides a very nice example of the richness of the chemical effects underlying the role of solvent on the excited states behavior of nucleobases, and, more in general, of photoexcited molecules in solution. To this purpose it is useful to discuss in further detail the curves in Figures 4 and 5.

**Tuning the Electronic Energies and Inducing State Mixings.** The first point to consider is obviously how solvent tunes the relative energy of the excited electronic states. Among them, the role played by the dark states should not be overlooked, since even if they are “silent” both in absorption and in emission they can constitute a very effective decay channel and eventually influence spectroscopic observables (for example, time-resolved excited-state absorption spectra). Our calculations of course confirm that the electronic states involving n/π\* transitions (i.e., the transfer of an electron from the LP of a carbonyl oxygen or a nitrogen atom toward the more diffuse π\* orbitals) are more sensitive to environmental effects, predicting that those transitions are disfavored by an increase of the solvent bulk dielectric constant and, especially, by the presence of solute/solvent hydrogen bonds. Nevertheless the case of uracil derivatives

allows us to put clearly in evidence how the importance of this feature is strictly related to the particular energy ordering of the molecular states. If, for example, the bright state is the lowest energy one already in the gas phase, it can be expected that, at least from this point of view, the excited-state lifetimes exhibit a quite modest dependence on the solvent. In this latter case (as for uracil) a hydrogen-bonding solvent, decreasing the S<sub>π</sub>–S<sub>n</sub> gap, could lead (for example owing to the presence of effective CI or to the so-called proximity effect<sup>67</sup>) to shorter excited-state lifetimes.

**Shaping the PES of Individual Excited States.** Inspection of Figures 4 and 5 clearly shows that solvent can significantly affect the shape of the PES associated to each single state. For example, the first part of the path toward S<sub>π</sub>-min in 5FU is flatter in acetonitrile than in water. Several microscopic effects can be responsible for this feature. Besides the interaction of different electronic states we discussed above, we can recall that the dipole moment depends on the molecular geometry and thus changes along the path on the excited-state surface: the polarity of the solvent obviously tunes the strength of this effect. Just to make an example, for 5FU in acetonitrile the excited-state dipole moment of the S<sub>π</sub> state is 10% smaller in S<sub>π</sub><sup>pla</sup>-min than in the FC region, whereas in water solution the dipole moment is almost constant along the path.

The height of the energy barrier on the S<sub>π</sub> path is another feature which is potentially sensitive to the nature of the solvent. Several experimental and computational studies have shown that, even if the decay mechanism differs from base to base, the radiationless ground-state recovery implies important ring deformations, bringing at least one substituent pseudoperpendicular to the ring plane, as in uracil,<sup>17–20,21–23</sup> cytosine,<sup>10,24–26</sup> and adenine.<sup>22,27–31</sup> However, we have shown that for uracils the energy barrier does not change significantly when going from acetonitrile to water. Furthermore all the experimental studies on DNA nucleobases agree in assigning extremely short excited-state lifetimes,<sup>1</sup> independent of the nature of the solvent. As a consequence, at least when treating polar solvents, this effect should play a minor role in determining excited-state lifetimes.

**Modulating Dynamical Effects.** Besides the “static effect” mentioned above, the excited-state lifetimes can be modulated by purely dynamical effects as well. For example, it is important to highlight that the existence of a region in the coordinate space where the bright and the dark states are close together, or even give rise to a conical intersection CI, is not sufficient to modify the photoexcited dynamics. It is indeed necessary that, as we found for uracil derivatives, the CI occurs in a region of the PES dynamically accessible to the wave packet in its motion after the electronic transition to S<sub>π</sub>.

Another important dynamical effect is related to the behavior of solute–solvent hydrogen bonds. As a matter of fact, while in uracil derivatives the equilibrium coordination geometry of the S<sub>π</sub> state is not very different from that in the ground state, that of the S<sub>n</sub> state involves more significant geometry shifts and, thus, more time should be required to reach the equilibrium.

Finally, as we have shown for uracil (Figure 4c,d), solvent can also modify the position of the crossing between electronic states. The system moving on the S<sub>π</sub> surface would then reach the crossing point with considerably different kinetic energy,

(67) Lim, E. C. *J. Phys. Chem.* **1986**, *90*, 6770.

depending on the solvent (not considering friction), and this can deeply modulate the transition probability to the  $S_n$  state.

Besides the effects we have concisely reviewed above, there are obviously other effects that can be present when studying solvent dependence of excited-state decay (e.g., the solvent modulation of the relative stabilities of different tautomers). However, we think that our considerations are sufficient to illustrate the complexity of the mechanisms modulating the dynamical behavior of excited states in the condensed phase, justifying the contradictory results of some of the previous study on this subject.

## 5. Concluding Remarks

In this paper we have reported the first comprehensive study of solvent effects on the excited-state behavior of the two lowest energy excited states of 2 pyrimidine nucleobases (uracil and 5-fluorouracil), both in acetonitrile and aqueous solution, analyzing their potential energy surfaces from the Franck–Condon region, through the excited-state minima, to the CI with the ground state.

The computed vertical excitations are in good agreement with their experimental counterparts and our PCM/TD-PBE0 calculations are able to reproduce the experimental acetonitrile/water absorption solvent-shift, indicating that the computational model we have employed is fully adequate to the study of nucleobases in solution. Analogously, our estimate of the fluorescence maximum is very close to its experimental counterpart, supporting the reliability of the recently developed TDDFT excited-state geometry optimizations in solution.

On the ground of the excited-state geometry optimizations and of the 2D maps connecting the FC and the minimum on  $S_\pi$ , we got interesting insights on the vibrational degrees of freedom most affected by the electronic transitions, and the indications provided by our computations agree with picture provided by RR experiments.<sup>63</sup>

To perform a more meaningful comparison between the excited-state decay mechanisms in two solvents with very different hydrogen-bonding power, we have located the CI between the bright and the ground state on supermolecules including four water molecules of the first solvation shell. To the best of our knowledge, this is the first time solvent molecules are taken into account at a quantum mechanical level in the study of conical intersections in a medium sized molecule. In any case, our calculations indicate that, independently of the nature of the solvent, *the key nuclear motion is the out-of-plane mode of the 5-substituent toward a “pseudoperpendicular” arrangement with respect to the molecular plane.* Therefore, our calculations predict that the basic mechanism of the ground-state recovery does not depend on environmental effects.

Our computations indicate instead that *solvent modulates the excited-state lifetime of uracils mainly by modifying the relative*

*energy and the interaction between their bright  $S_\pi$  and dark  $S_n$  states, which provides an extra decay channel for the wave packet moving on the  $S_\pi$  surface.* On this ground it is possible to understand how the excited-state lifetime of  $S_\pi$  changes depending on the solvent, and the predicted trend is in full agreement with the experimental one.

The results hereby presented provide a flavor of the richness and the complexity of the chemico-physical effects induced by the presence of the solvent. The solvent can indeed deeply affect both the shape of each single-state energy surface and their possible intersections. Since the final outcome depends also on the relative energy of the interacting states in the gas phase, we cannot expect that a given solvent affects the excited-state behavior always in the same direction. When acting on two different molecules the same microscopic effect (e.g., the relative destabilization of the  $S_n$  state in hydrogen-bonding solvents) can provide opposite results. This is the case of 5F and U showing that the experimental results can be interpreted only by taking into account the interplay between substituent and solvent effects. In such a scenario the integration of purposely tailored experimental and computational studies is of paramount importance.

Further work is of course necessary to judge the role of the solvent in this process, and we are currently extending our ultrafast fluorescence studies to other bases and to other solvent environments. At the same time, it would be highly desirable to perform dynamical simulations of the decay process. We think, however, that the results of the present study showing that the application of computational methods to the comparative study of different nucleobases in different solvents is a promising step toward a full understanding of the microscopic mechanisms underlying the photophysical behavior of nucleic acids and their constituents and, more in general, of photoexcited molecules in solution.

**Acknowledgment.** The authors thank CNRS for financial support within the framework of the European CERC3 program Photochemistry of Nucleic Acids and the Campus Grid at the University Federico II (Napoli) for computer resources.

**Supporting Information Available:** Geometries of the stationary points of the ground and excited states of 5FU and U in water and in acetonitrile; additional figures illustrating the frontier orbitals of uracils, the energy barrier on the path toward the CI with the ground state, the planar minimum of the  $S_\pi$  state, the PES of  $S_\pi$  and  $S_n$  in the region connecting the FC point, and the absolute  $S_\pi$  minimum; complete ref 62. This material is available free of charge via the Internet at <http://pubs.acs.org>.

JA0657861